©Operative Dentistry, 2021, **46-05,** 566-576

Influence of Incorporating Zirconium- and Barium-based Radiopaque Filler Into Experimental and Commercial Infiltrants

PR Pedreira • JE Damasceno • C Mathias • MAC Sinhoreti • FHB Aguiar • GM Marchi

Clinical Relevance

Important progress has been made in researching the radiopacity of resin infiltrants to determine their efficacy, since the infiltrant currently available on the market is not radiopaque. Adequate radiopacity would allow clinicians to confirm the penetration and efficacy of the infiltrant.

SUMMARY

Objectives: To evaluate how adding different concentrations of particles (barium or zirconium oxide 25%/45% by weight) to a commercial infiltrant (Icon) and an experimental infiltrant influences cohesive strength (CS), degree of conversion (DC), water sorption (WS), solubility (SL), radiopacity, and penetration depth.

Methods and Materials: Microtensile CS (n=10) was evaluated using a universal testing machine. DC (n=5) was evaluated in a Fourier-transform infrared spectrometer. Polymerized samples were dissected, weighed, and stored to obtain the final mass for WS and SL tests (n=10). Radiopacity analysis (n=5) was performed using a digital radiography system. Penetration depth analysis (n=5) was performed by confocal laser scanning microscopy. Analyses were performed using the R program, with a significance level of 5%, except for the penetration depth analyses, which were evaluated only qualitatively.

Results: The groups with 45% zirconium showed greater CS values, regardless of the infiltrant. Among the groups with no particle addition, those of the experimental infiltrant

---

*Priscila Regis Pedreira, Department of Restorative Dentistry, Piracicaba Dental School, State University of Campinas, Piracicaba, SP, Brazil

Janaina Emanuela Damasceno, Department of Restorative Dentistry, Piracicaba Dental School, State University of Campinas, Piracicaba, SP, Brazil

Caroline Mathias, Department of Restorative Dentistry, Piracicaba Dental School, State University of Campinas, Piracicaba, SP, Brazil

Mário Alexandre Coelho Sinhoreti, Department of Restorative Dentistry, Piracicaba Dental School, State University of Campinas, Piracicaba, SP, Brazil

Flávio Henrique Baggio Aguiar, Department of Restorative Dentistry, Piracicaba Dental School, State University of Campinas, Piracicaba, SP, Brazil

Giselle Maria Marchi, Department of Restorative Dentistry, Piracicaba Dental School, State University of Campinas, Piracicaba, SP, Brazil

Corresponding author: Av Limeira, 901, PO Box 52 Piracicaba, SP, Brazil, CEP 13414-903; e-mail: priscilaregis1@hotmail.com

https://doi.org/10.2341/20-020-L

presented higher DC than those of Icon. The experimental infiltrant presented lower WS than Icon. All groups had SL below the ISO recommended levels. Radiopacity higher than 2.24 mmAl (enamel radiopacity) was observed only in the groups with 45% zirconium. All the groups achieved similar penetration depth, but the groups containing experimental infiltrant appear to have had longer tag extensions.

Conclusions: Addition of 45% of zirconium presented good results for CS and WS, as well as SL below the ISO recommended standard, adequate radiopacity, and penetration depth similar to the other groups.

INTRODUCTION

A reduction in the incidence of dental caries has been observed in recent years, especially among children and adolescents.[1] However, the disease is still considered a public health problem, since dental caries is one of the most common diseases affecting the population.[1,2] A number of preventive measures implemented in the last decades has led to a decline in dental caries lesions.[3] However, active white spots—the first clinical observation of caries progression—are still frequent. They are caused by the high concentration of acids produced by bacteria in the biofilm and associated with poor hygiene.[4] An active white spot lesion (WSL) is an enamel subsurface demineralization that is noncavitated and that can be remineralized.[2,5]

The treatments of choice for incipient carious lesions are minimally invasive procedures adopted to avoid dental tissue removal. Noninvasive methods, topical fluoride application, and oral hygiene are resources used to promote the remineralization of incipient lesions.[2,6,7] However, these procedures require the cooperation of patients to ensure successful treatment. In addition, these methods remineralize only the surface of the lesion.[8]

Since patients are often not cooperative, other alternatives have been put into place to prevent dental caries progression in the initial phase of lesion development. The low-viscosity resin infiltration technique is one such option that has been used successfully in dentistry.[3] The principle of resin infiltration is to perfuse porous enamel by capillary action, thus interrupting the demineralization process and paralyzing the carious lesion.[9] Icon is a low-viscosity, commercially available resin infiltrant consisting of a methacrylate resin matrix, initiators, and additives.[3] It is applied mainly to initial white spots on smooth and proximal tooth surfaces.[3,4]

Given the promising studies conducted on the effectiveness of Icon infiltration and the importance of avoiding tooth wear when treating WSLs, some studies have tested infiltrant compositions according to different combinations of monomers, diluents, and solvents, seeking to improve the only commercially available infiltrant in regard to penetration depth and mechanical properties.[3,10-13] One of these formulations was studied by Mathias and others,[14] based on 25% ethoxylatedbisphenol A dimethacrylate (*Bis*-EMA), 75% triethylene glycol dimethacrylate (TEGDMA), 0.5% camphorquinone (CQ), and 1% ethyl 4-dimethylaminobenzoate (EDAB), with favorable results regarding degree of conversion (DC), sorption, and solubility (SL).

However, the disadvantage of a resin infiltrant is that it is radiolucent. According to the American Dental Association (ADA), radiopacity is an essential property of all restorative materials and one of the requirements of a dental material. Material with adequate radiopacity allows secondary caries and marginal defects to be detected, as well as missing contact points with adjacent teeth, improves restoration contours, and distinguishes caries from restorative material and surrounding tooth structure.[15-17] In addition, radiopacity is not only associated with the amount of filler present in the material but also with the type of radiopaque additives in inorganic fillers.[16] For example, most restorative resins can be visualized well in a radiographic diagnosis, albeit dependent on their composition.[16,18] The elements composing resin radiopacification have a high atomic number, such as barium oxide, lanthanum, strontium, zirconium, zinc, yttrium, and ytterbium, which vary greatly in their concentrations [18]. According to the literature researched, the most commonly used components are barium oxide and zirconium particles, which ensure the good radiographic results of radiopacity composites [17,18].

Both barium and zirconium particles consist of colorless, insoluble crystals in water, and are available in white powder form. The lower the particle size, the lower the viscosity, and the greater the penetration depth, according to Lee and others.[19] Barium oxide particles have an average size of 0.7 um, whereas zirconium oxide particles are <100 nm, on average. The composition of the only commercially available infiltrant lacks radiopacity in its composition. Consequently, penetration of the infiltrant in the lesion cannot be visualized at an

Table 1: *Description of Experimental Group Composition*

INFILTRANT GROUP	COMPOSITION
CC (Comercial Control)	Icon
I25B	Icon, 25% Barium Oxide
I45B	Icon, 45% Barium Oxide
I25Z	Icon, 25% Zirconium Oxide
I45Z	Icon, 45% Zirconium Oxide
EC (Experimental Control)	25% *Bis*-EMA, 75% TEGDMA, 0,5% CQ, 1% EDAB
E25B	25% *Bis*-EMA, 75% TEGDMA, 0.5% CQ, 1% EDAB, 25% Barium Oxide
E45B	25% *Bis*-EMA, 75% TEGDMA, 0.5% CQ, 1% EDAB, 45% Barium Oxide
E25Z	25% *Bis*-EMA, 75% TEGDMA, 0.5% CQ, 1% EDAB, 25% Zirconium Oxide
E45Z	25% *Bis*-EMA, 75% TEGDMA, 0.5% CQ, 1% EDAB, 45% Zirconium Oxide

Description of acronyms used in the table: Bis-EMA, ethoxylatedbisphenol A dimethacrylate, ESSTECH; TEGDMA, triethylene glycol dimethacrylate, Aldrich; CQ, camphorquinone, Aldrich; EDAB, ethyl-4-dimethylamino benzoate, Aldrich.

adequate depth, and its efficacy and ability to stabilize the lesion cannot be ascertained.

In view of the scarcity of studies and the need for an infiltrant that has radiopacity, adequate physicomechanical properties, and ability to penetrate the demineralized enamel zone, this study proposed to evaluate the incorporation of barium oxide and zirconium particles into commercial and experimental infiltrants to promote radiopacity, assess resulting physical properties, and improve penetration.

METHODS AND MATERIALS

Infiltrant Preparation

The experimental infiltrant was manipulated in a laboratory with yellow light, and controlled humidity and temperature. The monomeric base used was *Bis*-EMA and TEGDMA. A CQ and a tertiary amine ethyl-4-dimethylamino benzoate (EDAB) photoinitiator system were also added. Barium oxide and zirconium particles were incorporated into the experimental infiltrant and Icon (XXX). The incorporation was performed using a magnetic stirrer for 24 hours and an ultrasonic vessel for 30 minutes, in the concentrations shown in Table 1, all in percentage by weight. The experimental infiltrants were stored individually and kept under refrigeration at 4°C.

Cohesive strength (CS)

A microtensile test was used to evaluate cohesive strength (CS). A ten bar-shaped matrix (8×1×1 mm) was used to make silicone impressions (Scan Putty, Yller) to obtain 10 specimens for each group tested. The specimens were photoactivated by an LED light source (Valo, Ultradent, xxx, power density of 1000 mW/cm^2, 395-480 nm) for 40 seconds, and stored in an incubator at 37°C for 24 hours. Each specimen was fixed with cyanoacrylate glue (Superbonder, Locitec, São Paulo, SP, Brazil) to a metal microtensile device, coupled to a universal test machine (Instron 4411, Norwood, MA, USA). The machine was operated at a speed of 1 mm/minute, until the stick ruptured. The fracture area was measured individually using a digital caliper to calculate the stress and rupture of each specimen in MPa.

Degree of Conversion (DC)

DC analyses (GC, in %, n=5) were performed by Fourier-Transform Infrared Spectroscopy (Vertex 70 Spectrometer, Bruker, Billerica, MA, USA) in transmission mode. Two readings were performed: one of the unpolymerized material and the other of the same material immediately after photoactivation with an LED light source (Valo) for 40 seconds. The conversion was obtained by recording the methacrylate absorption peak (6165/cm), before and after polymerization. The baseline technique[20] was drawn by the program itself and was used to calculate the DC.

Water sorption (WS) and Solubility (SL)

Water sorption (WS) and solubility (SL) tests were performed according to ISO 4049/2009, except on specimen size. A Teflon matrix with a cylindrical shape was used to make a silicone matrix (Scan Putty, Yller). The infiltrant was deposited in this matrix to obtain test specimens in the form of a disc (5×1 mm, n=10), which were then polymerized with an LED light source (Valo) for 40 seconds, placed in a desiccator and stored in an incubator at 37°C.

The test specimens were weighed daily on an analytical balance (Shimadzu - AUW220D, Tokyo, Japan), at 24-hour intervals until constant mass (m_1) was obtained, with a variation of less than 0.002 mg. The thickness and diameter of each specimen was measured with a digital caliper (Mitutoyo, Japan) to calculate the volume (mm^3). Afterwards, the specimens were stored at 37°C in closed Eppendorf tubes containing 1.5 mL of distilled water. After 7 days in storage, the Eppendorf tubes were removed from the incubator and left at room temperature for 30 minutes. The specimens were washed in running water, dried gently with absorbent paper, and reweighed on an analytical balance to obtain m_2. The samples were then dried in a desiccator containing silica gel and reweighed daily to obtain a new constant mass (m_3). The WS and SL values were calculated by two separate formulas ($S_o=m_2-m_3/V$ and $SL=m_1-m_3/V$).

Radiopacity

The radiopacity analysis was performed by making a disc-shaped specimen (5×1 mm, n=5) from a silicone matrix. The specimens were photoactivated with an LED light source (Valo) for 40 seconds and stored at 37°C for 24 hours. The Kodak Dental Systems digital radiography system (RVG 5000, Eastman Kodak Company, Rochester, NY, USA) was used to perform the analysis. This system has a sensor with electro-optical features of three juxtaposed blades: scintillator crystal, fiber optic, and filler coupled device (CCD). The blades produce an electrical signal that generates an image with a real resolution of 14 pl/mm and a real image receiver resolution of 27.03 pl/mm. The specimens were positioned together with the film at the center of the sensor, and the aluminum density scale and a tooth on the side to compare the density. The radiographic apparatus cylinder (Timex 70 E, Gnatus, Osasco, SP, Brazil), 70 kVp and 7 mA, was positioned perpendicular to the film, specimen, scale, and tooth at a distance of 5 cm, using an exposure time of 0.05 seconds.

The digital image provided optical density values in pixels at the center of each specimen, of each step of the scale, and of the points equidistant from the right and left. This allowed obtaining an average of the radiographic density value. Grayscale comparisons were made to assess and compare the radiopacity level, as evaluated by the histogram contained in the Adobe Photoshop software. The following equation was used to transform the data to mm a [21]:

$(A\times0.5)/B+$mm to immediately preceding radiographic density of the material (DRM)
A = Radiographic density of the material (DRM) – radiographic density of the aluminum increment immediately preceding DRM;
B = Radiographic density of the aluminum increment immediately after DRM–Radiographic density of the aluminum increment immediately preceding DRM;
0.5 = 0.5-mm increment of the aluminum scale.

The density of each specimen was compared with the dentin density (1.23 mmAl) and the enamel density (2.24 mmAl), represented by the thickness of the aluminum density scale of 1 mm and 2 mm, respectively. Bear in mind that this thickness had to be equivalent to or greater than these respective values, in order to determine the most adequate concentration to distinguish the material.

Penetration Depth

Preparation and Selection of Test Specimens—Sixty human molars were cleaned thoroughly with a prophylaxis brush (Microdont, São Paulo, Brazil) and pumice slurry (AAF do Brasil, Londrina, Brazil) to remove residues and then stored in a 0.1% thymol solution. Tooth roots were removed and discarded. Next, fragments (n=50) were obtained from the enamel portion of buccal and lingual/palatine faces of 60 teeth. The enamel surface of each specimen was ground flat and polished with waterproof silicon carbide papers (600-, 1200-, and 2000-grit; Sands, Norton, Guarulhos, SP, Brazil) under refrigeration, and then polished with felt disks and a diamond solution (1 μm, Buehler). The fragments were covered with two layers of resistant nail varnish (Colorama, São Paulo, Brazil), except in the polished enamel area (4×4 mm). They were stored individually in distilled water at 37°C. The resulting specimens were then tested. The initial microhardness average was obtained with a microdurometer (HMV-2000; Shimadzu Corporation, Tokyo, Japan) using three measurements 100 μm from each other, as of the center of the surface. The sample specimens with a mean value of 360 ± 28 were selected.

Simulation of the Initial Enamel Caries Lesion—The selected specimens were submitted to a caries lesion simulation in enamel. Activity in the oral cavity was simulated using a demineralizing solution (2.2 mmol $CaCl_2$, 2.2 mmol NaH_2 PO_4, and 50 mmol acetic acid, adjusted to pH 4.5 with NaOH).[22] The demineralization cycle was simulated by immersing the specimens individually into 50 ml of solution for 16 hours at 37°C, washing them with distilled water, and then keeping them in *Tris* buffer solution (0.1 M HCl, pH 7.0) at 37°C. Two other groups were made to evaluate the correct demineralization of the test specimens: one positive control and one negative control.

Penetration Depth Evaluation—After the caries lesion simulation was performed, the specimens were submitted to different commercial and experimental infiltrants. Ten study groups (n=5) of the infiltrants were used to evaluate penetration depth.

Table 2: *Mean and standard deviation of cohesive strength (CS), degree of conversion (DC), sorption and solubility (SL), according to the infiltration and concentration of the barium and zirconium particles*

Filler concentration	**0%**	**Barium 25%**	**Barium 45%**	**Zirconium 25%**	**Zirconium 45%**
Cohesive Strength					
Icon (DP)	40.87 (7.76)Ab	48.18 (11.73)Ab	51.21 (9.3)Aab	46.51 (9.99)Ab	58.32 (7.30)Aa
Experimental (DP)	47.94 (8.82)Ab	44.74 (8.96)Ab	50.16 (5.60)Aab	45.20 (4.79)Ab	54.48 (10.59)Aa
Degree of Conversion					
Icon (DP)	60.50 (7.55)Bb	85.69 (1.95)Aa	85.26 (1.38)Aa	77.70 (1.95)Aa	68.63 (3.43)Ab
Experimental (DP)	77.40 (1.48)Aa	75.75 (1.24)Ba	76.92 (1.89)Ba	69.29 (12.34)Bb	68.12 (8.09)Ab
Sorption					
Icon (DP)	57.14 (3.12)Aab	59.08 (3.08)Aa	54.30 (6.73)Ab	57.11 (4.80)Aab	54.83 (3.37)Ab
Experimental (DP)	36.90 (2.77)Bb	35.03 (2.56)Bbc	33.98 (2.27)Bc	39.54 (2.78)Ba	36.55(3.72)Bb

Different uppercase letters indicate statistical difference in the same column for each test, different lowercase letters indicate statistical difference in the same line $p < 0.05$

This was performed by conditioning the enamel with 15% hydrochloric acid for 120 seconds, according to the manufacturer's recommended protocol (Icon Etch, DMG, Hamburg, Germany). The enamel was washed with a water jet for 120 seconds and then dried with air jets for 15 seconds. The teeth were washed again for 30 seconds and immersed in a 0.1% Rhodamine B ethanolic solution (Sigma–Aldrich, Steinheim, Germany) for 12 hours to fill all accessible pores with red fluorophore, as a protocol for visualization in a confocal microscope (only).

After removal of the pigment solution with a water jet, the specimens were dried with compressed air for 30 seconds, immediately before the resinous infiltration. Icon Dry (99% ethanol) was applied for 30 seconds, and the infiltrants were applied for 180 seconds, according to the manufacturer's recommendation. Afterwards, the specimens were photoactivated for 40 seconds using an LED photoactivator (Valo). The infiltrant was reapplied for 60 seconds, and photoactivation was performed for 40 seconds, as recommended by the manufacturer.

The resin-infiltrated blocks were sliced perpendicular to the surface of the enamel lesion with a diamond disc and polished (600-, 1200-, and 2000-grit; sandpaper, Norton) with water to produce approximately 1.0-mm thick fragments. Unbound red fluorophore was removed by leaving the slices in a 30% hydrogen peroxide solution for 12 hours, according to the confocal microscopy protocol. The lesion regions in which no infiltration occurred were evaluated by immersing the specimens in a 100-μM sodium fluorescein ethanolic solution (NaFl; Sigma–Aldrich, St. Louis, MI, USA) for 180 hours and subsequently washing them with deionized water for 10 seconds. After the specimens were prepared, they were evaluated by Confocal Laser Scanning (Leica, TCS NT; Leica, Heidelberg, Germany) with a 63 × 1.4 NA objective. The dual fluorescence mode was used with the oil-immersion objective, to enable fluorescence to be detected simultaneously (Rhodamine B: Ex 568-nm, 590-nm long-pass filter; fluorescein sodium: Ex 488-nm, 520/50-nm band-pass filter). Penetration depth of the images obtained was evaluated qualitatively to check for penetration.

Statistical Analysis—Initially, descriptive and exploratory analyses were performed, since the data did not meet the assumptions of a parametric analysis. Generalized linear models were then applied considering the following factors in the model: the infiltrant, the particles, and the interaction among them. All the analyses were performed using the R* program [*R Core Team (2018); R Foundation for Statistical Computing, Vienna, Austria], considering a 5% level of significance.

RESULTS

Regarding CS, the interaction between the infiltrating factors and the particles was not significant ($p>0.05$). Moreover, there was no significant difference between the Icon and experimental infiltrants ($p>0.05$), as shown in Table 2. The resistance in the 45% zirconium group was significantly higher than that of the 25% zirconium, the 25% barium, or the control groups ($p<0.05$), regardless of the infiltrant. Comparing the CC (with particle addition) and EC (without its addition) groups, EC had higher DC than CC ($p<0.05$) (Table 2). The groups with Icon presented higher DC ($p<0.05$) than the groups with the addition of 25% barium and of 25% zirconium, respectively. In the I45Z and E45Z groups, there was no significant difference between the two infiltrants ($p>0.05$). In regard to Icon, it was observed that the I45Z group did not differ from the control group, and that the other groups presented significantly higher averages ($p<0.05$) than the control group. In the

Table 3: *Mean and Standard Deviation of Radiopacity (mm Al) Values, According to the Infiltration and Concentration of the Barium and Zirconium Particles, in Comparison with the Enamel and Dentin Radiopacity Values*

Particles	Infiltrant	
	Icon	Experimental
Control	0.47 (0.04) Ae	0.49 (0.03) Ae
25% Barium	0.88 (0.07) Ad	0.84 (0.05) Ad
45% Barium	1.15 (0.22) Ac	1.17 (0.18) Ac
25% Zirconia	1.53 (0.24) Ab	1.82 (0.40) Ab
45% Zirconia	2.77 (0.27) Aa	2.78 (0.20) Aa

Averages followed by different letters (uppercase in the same line and lowercase in the same column) differ among one another ($p \leq 0.05$). p(Infiltrant)=0.5447; p(Particles)<0.0001; p(Infiltrant×Particles)=0.4528

case of the commercial infiltrant, lower DC values were observed in the zirconium groups ($p<0.05$).

The experimental infiltrant presented lower WS than Icon, irrespective of particle concentration ($p<0.05$) (Table 2). As for Icon, the I25B group presented significantly higher WS than the I45B or zirconium ($p<0.05$) groups. As for the experimental infiltrant, the highest WS was observed in the E25Z group, whose concentration differed significantly from the other particle concentrations ($p<0.05$). As for the control groups and those with the addition of 25% barium, a higher SL was observed in the experimental group ($p<0.05$) (Table 2). Regarding Icon, greater SL was observed in the I25Z and I45Z groups, and the SL was significantly higher at the 45% concentration ($p<0.05$). Regarding the experimental infiltrant, the E45Z group presented higher SL than groups E25B and E45B, $p<0.05$.

In regards to radiopacity, Table 3 indicates that there was no significant interaction between the infiltrants and the particle concentration ($p>0.05$). Therefore, there was no significant difference in radiopacity between Icon and the experimental infiltrants, regardless of the barium oxide or zirconium particle concentrations ($p>0.05$). Greater radiopacity was observed when zirconium was added ($p<0.05$), pointing out that it was significantly higher in the 45% concentration, regardless of the infiltrant. Figure 1 shows the radiopacity of the CC, I25B, I45B, I25Z, and I45z (Figure 1a), and of EC, E25B, E45B, E35Z, and E45Z (Figure 1b) specimens, as well as a tooth fragment in relation to the aluminum scale.

The images of the degree of homogeneity of penetration of the infiltrating materials in the lesion body were evaluated qualitatively using confocal microscopy (Figure 2). All the groups obtained similar depth of penetration, but the image representing the penetration depth of the experimental infiltrants suggests that the tags of the infiltrants were not only longer but also more homogeneously prolonged, thus possibly achieving better penetration depth.

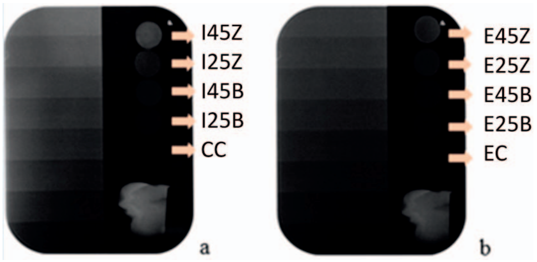

Figure 1. *a) Shows the radiopacity of specimens of the CC, I25B, I45B, I25Z, and I45z groups, compared with the tooth and aluminum scale; b) shows the radiopacity of specimens of the EC, E25B, E45B, E35Z, and E45Z groups, compared with the tooth and aluminum scale.*

DISCUSSION

The aim of this study was to evaluate how adding barium oxide and zirconium particles to experimental and commercial infiltrants would influence the physical properties of the infiltrants, to give them radiopacity. Percentage concentrations by weight of 25% and 45% barium oxide were added to the infiltrants, similar to the concentrations evaluated in the study by Askar and others.[4] These same concentrations were used for the zirconium oxide particles.[23]

The reason for using small particle sizes (0.7 µm and <100 nm) was based on the greater possibility of penetrating demineralized microporosities, since the outer layers of demineralized enamel in *in vitro* artificial lesions have microporosities with a diameter between 27 and 44 µm and a total demineralization depth ranging from 93 to 219 µm, according to Groeneveld and Arends.[24] On the other hand, Cochrane and others[25] have shown that natural lesions of enamel caries are characterized by microporosities with a smaller diameter, ranging from 35 to 130 µm.

Overall, filler particles give resinous material directly proportional resistance and viscosity properties. In other words, the higher the amount of filler particles, the greater the physical properties of the resin compound, resulting in higher resistance to material deformation and higher viscosity.[26,27] Icon presented a lower CS value without the addition of filler particles, compared to the other groups tested

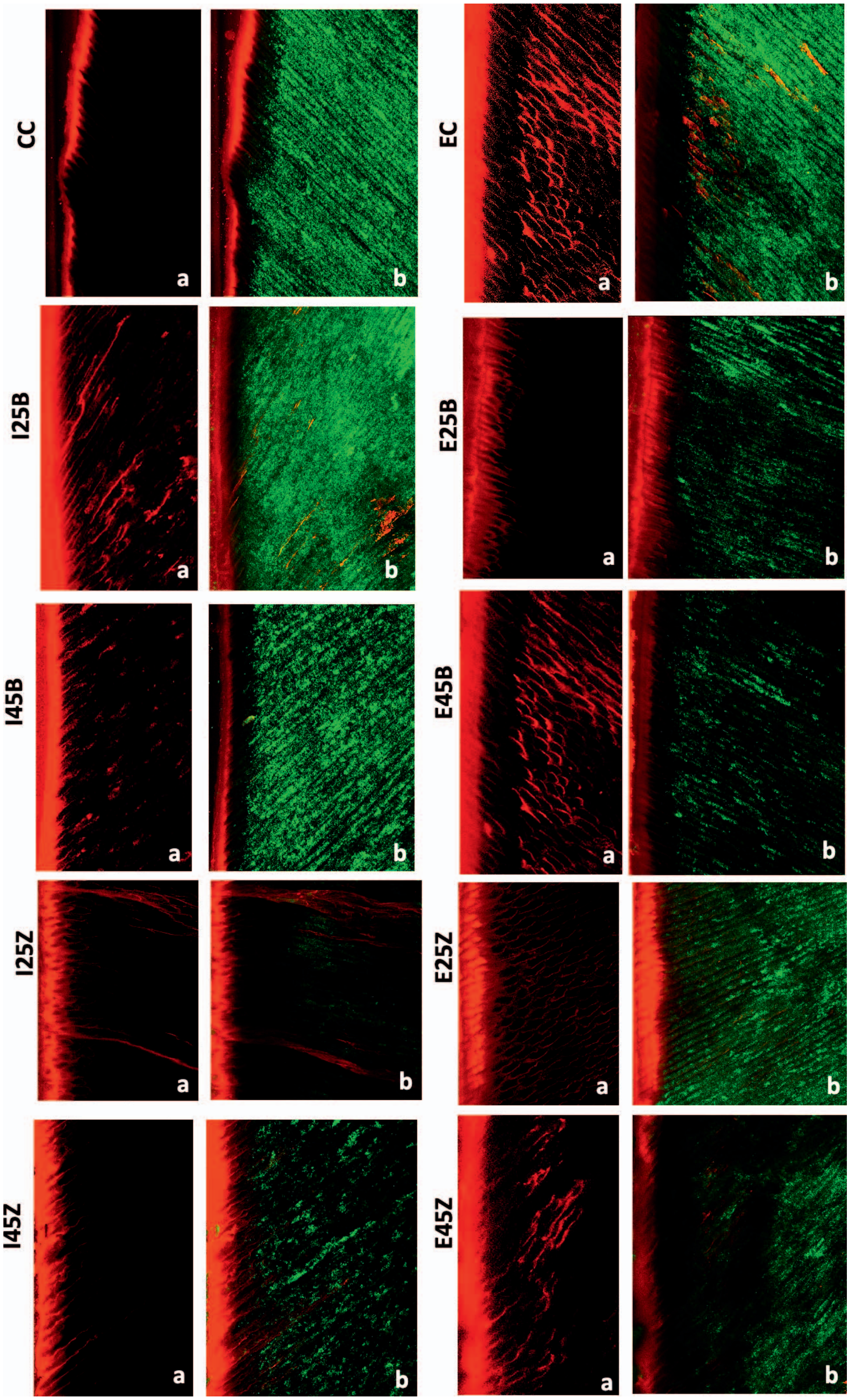

Figure 2. *Penetration depth in dual fluorescence mode of groups CC, EC, I25B, E25B, I45B, E45B, I25Z, E25Z, I45Z, E45Z. a) Colored resinous material infiltrated in red. b) Interaction between colored resin material (red) and demineralized porous structures in green. CC showed superficial penetration compared with EC. EC showed longer tags and a thicker red layer; resinous material may have been retained in that region of the lesion surface. I25B showed penetration with few extended tags. E25B showed more homogeneous tags, but not as deep. I45B showed superficial penetration with few extensions. E45B showed longer tags and a thicker red layer, resinous material may have been retained in that region of the lesion surface. I25Z showed a thicker layer of more intense red on the surface, possibly due to the presence of particles of zirconia and resin that may have been trapped in this region. E25Z showed longer and more homogeneous tags, with a thicker layer, similar to that of I25Z. I45Z showed superficial penetration with a thicker red layer; resinous material may have been retained in that region of the lesion surface. E45Z showed longer tags and a thicker red layer, also similar to I45Z.*

in this study (Table 2). This result can be attributed to the presence of a relatively high amount of TEGDMA, as well as the absence of filler particles in its composition.[26-28] The highest values found for CS were groups with 45% addition of zirconium (Table 2); this is because a larger number of particles are needed to fill equal volumes of filler with smaller-sized particles (<100 nm). Thus, the surface area may have increased, and this may have resulted in greater interaction between the resin matrix and filler particles, and among the filler particles themselves, thus increasing the resistance.[19]

A high DC is often correlated with better mechanical properties of restorative composites, thus reducing possible risk of fractures and material wear in intraoral functions.[28] The lowest DC was found for Icon (Table 2)—a result that can be attributed to the excessive amount of TEGDMA in its composition (>90% by weight). This finding agrees with previous studies, which have shown that the DC decreases as the concentration of TEGDMA increases (>70% by weight),[29-31] TEGDMA has a high DC; however, formation of the polymer chain does not always occur. In addition, the absence of strong intermolecular secondary bonds as well as the presence of aromatic rings results in properties inferior to those of other monomers.[32] The EC group presented a higher DC value than IC (Table 2). This may have been caused by the presence of *Bis*-EMA. The molecular structure of *Bis*-EMA is similar to that of *Bis*-GMA, differing in regard to the absence of hydroxyl groups. This absence induces the nonformation of hydrogen bonds and reduces the viscosity of *Bis*-EMA compared to *Bis*-GMA. In this respect, the research literature has shown that higher DC can be achieved by using specific concentrations of monomers with lower viscosity, such as *Bis*-EMA.[28]

Addition of 45% zirconium led to a reduction in DC in both the experimental and Icon groups (Table 2). This corroborates the findings of Halvorson and others,[33] which concluded that the DC decreased when there was an increase in the number of filler particles. This can be explained by the mobility of resin monomers that can be restricted at the surface of the composite, leading to a decrease in molecular and radical motility, and resulting in lower DC. However, the influence of the filler particle on the DC may be more related to the size of the particle surface area than to the number of filler particles.[33,34] The increase in DC in groups I25B and I45B can be attributed to barium having a larger particle size than zirconium. In contrast, the addition of barium to the experimental groups had no effect (Table 2).

The mechanical properties of resinous materials can be altered due to degradation by water, and the polymerization quality of these materials may be related to the chemical characteristics of monomers.[35] Resin-based dental materials can absorb water and other fluids from the oral environment, such as WS, and may also release components into the oral environment, such as SL.[28] According to ISO 4049/2009, composites can be indicated as restorative materials only if they have WS less than or equal to 40 μg/mm^3 and SL less than or equal to 7.5 μg/mm^3 in a period of 7 days of storage. High WS and SL values can trigger chemical and physical processes that may result in detrimental effects on the structure and function of dental polymers.[28]

All groups containing Icon presented a higher than recommended WS, whereas the groups containing the experimental infiltrant presented values lower than 40 μg/mm^3 (Table 2). Thus, we may infer that the lower DC obtained with Icon may have influenced CS and WS values negatively. However, the lower values of WS obtained with the experimental infiltrants, compared to Icon, may be due to the *Bis*-EMA in their composition. This hypothesis is in agreement with an earlier study that showed low WS for *Bis*-EMA, which has a relatively higher DC value and a more hydrophobic character than *Bis*-GMA[28]. When a polymer is placed in water, hydrogen bonds are formed by water in conjunction with polymeric polar groups, such as hydroxyl and carbonyl. This condition may disrupt the intercellular interaction of the polymer.[35] Since *Bis*-EMA has no hydroxyl groups, but has ether groups instead, this effect may not occur, resulting in lower water solids.[35] In addition, TEGDMA—probably the largest component of Icon—can be homopolymer- or copolymer-free, forming a polymer chain prone to chemical degradation, especially in acidic environments.[32]

All the groups obtained lower SL values than that recommended by ISO (Table 2). This finding of the present study contradicts that of the study by Sfalcin and others,[28] who found the SL value of Icon to be 49 μg/mm^3. However, the study by Inakagi and others[35] also found lower SL values (5.76 μg/mm^3) than those recommended by ISO. However, in both studies, photopolymerization was carried out for 60 seconds, unlike the present study that used 40 seconds.

The groups that obtained higher radiopacity values than those of enamel (2.24 mmAl) were the

I45Z and E45Z groups, whereas those that obtained higher radiopacity values than those of dentin (1.23 mmAl) were I25Z and E25Z (Figure 1). Higher radiopacity was found in the I45Z and E45Z groups, where there was a greater quantity of filler particles, since the radiopacity of a material increases as the filler particle concentration increases in higher atomic number, as has been demonstrated in other studies.[15-17] In this study, zirconium showed higher radiopacity when compared to barium in the same proportions (Figure 1), corroborating the findings of previous studies.[15,36,37] The amounts of 25% and 45% barium were not sufficient to obtain values of radiopacity above that recommended by the International Organization for Standardization (ISO 4049/2009). Studies by Watts [38] and Van Dijken and others[39] have shown that 70% of filler particles in volume by weight are required to obtain radiopacity values higher than those of enamel, whereas the percentage of high atomic number particles (radiopacifiers) may be greater than 20%. Generally, there are several particles with a high atomic number in composite resins; this may explain why barium may not have reached the required radiopacity value. However, this was the first study to test radiopacity in infiltrants. Future studies should analyze and confirm these important findings.

The ability of carious lesions to penetrate the teeth was evaluated qualitatively using confocal microscopy images (Figure 2). The addition of filler particles to the experimental and commercial infiltrant groups resulted in a similar penetration depth, but the experimental group had longer resin tags. That is to say, the addition of the particles may not have influenced the penetration of the infiltrants. The high permeability of the resin infiltrant may be attributed to the low viscosity of TEGDMA, as well as its low molecular weight, characteristics that allowed higher infiltration penetration in comparison with other materials, such as sealants and adhesives.[32]

The proposal of an infiltrant that can penetrate carious enamel lesions is promising, and the confirmation of radiographic success is of paramount importance. This study featured pioneering research into the addition of filler particles with the objective of providing infiltrant material with radiopacity, without altering its physical properties detrimentally. Further studies should expand on these findings by testing other percentages and other types of elements of high atomic number, and even by mixing two radiopacifying particles, as has been proposed in some studies.

In addition, it is important to point out that, depending on filler size, these radiopaque particles could have a negative influence due to resin staining used to mask WSLs in the vestibular region, as a result of polishing.[27] However, radiopaque particles are not as important to the vestibular as they are to the interproximal region. Therefore, there could be two types of infiltrants, which would be supplied in two different packages, considering that their application tips are different.

CONCLUSION

According to the results obtained in this study, it was possible to conclude that addition of 45% of zirconium presented good results for CS and WS, SL below the recommended standard, and adequate radiopacity, and penetration depth similar to that of the other groups.

Acknowledgements

The authors thank Prof Dr Roberto Braga of USP for kindly granting one of the equipment to perform one of the tests.

Regulatory Statement

This study was conducted in accordance with all the provisions of the human subjects' oversight committee guidelines and policies of Committee of Ethics in Research of Piracicaba Dental School—UNICAMP. The approval code issued for this study is 2,772,954.

Conflict of Interest

The authors of this manuscript certify that they have no proprietary, financial, or other personal interest of any nature or kind in any product, service, and/or company that is presented in this manuscript.

(Accepted 26 November 2020)

REFERENCES

1. Marcenes W, Kassebaum NJ, Bernabé E, Flaxman A, Naghavi M, Lopez A, & Murray CJ (2013) Global burden of oral conditions in 1990–2010: A systematic analysis *Journal of Dental Research* **92(7)** 592-597.
2. Paula AB, Fernandes AR, Coelho AS, Marto CM, Ferreira MM, Caramelo F, do Vale F, & Carrilho EJ (2017) Therapies for white spot lesions: A systematic review evidence-based dental practice **17(1)** 23-38. doi: 10.1016/j.jebdp.2016.10.003
3. Golz L, Simonis RA, Reichelt J, Stark H, Frentzen M, Allam JP, Probstmeier R, Winter J, & Dominik K (2016) In vitro biocompatibility of ICON and TEGDMA on human dental pulp stem cells *Dental Materials* **32(8)** 1052-1064.
4. Askar H, Lausch J, Dörfer CE, Meyer-Lueckel H, & Paris S (2015) Penetration of micro-filled infiltrant resins into artificial caries lesions *Journal of Dentistry* **43(7)** 832-838.
5. Meyer-Lueckel H & Paris S (2008) Improved resin infiltration of natural caries lesions. *Journal of Dental Research* **87(12)** 1112-1116.

6. Young DA & Featherstone JD (2010) Implementing caries risk assessment and clinical interventions *Dental Clinics of North America* **54(3)** 495-505.
7. Ceci M, Rattalino D, Viola M, Beltrami R, Chiesa M, Colombo M, & Poggio C (2017) Resin infiltrant for non-cavitated caries lesions: Evaluation of color stability *Journal of Clinical and Experimental Dentistry* **9(2)** e231-e237.
8. Mandava J, Reddy YS, Kantheti S, Chalasani U, Ravi RC, Borugadda R, & Konagala RK (2017) Microhardness and penetration of artificial white spot lesions treated with resin or colloidal silica infiltration *Journal of Clinical and Diagnostic Research* **11(4)** ZC142-ZC146.
9. Lasfargues JJ, Bonte E, Guerrieri A, & Fezzani L (2013) Minimal intervention dentistry: Part 6. Caries inhibition by resin infiltration *British Dental Journal* **214(2)** 53-9. doi: 10.1038/sj.bdj.2013.54
10. Araújo GS, Sfalcin RA, Araújo TG, Alonso RC, & Puppin-Rontani RM (2013) Evaluation of polymerization characteristics and penetration into enamel caries lesions of experimental infiltrants *Journal of Dentistry* **41(11)** 1014-1019.
11. Paris S, Meyer-Lueckel H, Cölfen H, & Kielbassa AM (2007) Resin infiltration of artificial enamel caries lesions with experimental light curing resins *Dental Materials Journal* **26(4)** 582-588.
12. Ekstrand KR, Bakhshandeh A, & Martignon S (2010) Treatment of proximal superficial caries lesions on primary molar teeth with resin infiltration and fluoride varnish versus fluoride varnish only: Efficacy after 1 year *Caries Research* **44(1)** 41-46.
13. Paris S, Hopfenmuller W, & Meyer-Lueckel H (2010) Resin infiltration of caries lesions: an efficacy randomized trial *Journal of Dental Research* **89(8)** 823-826.
14. Mathias C, Gomes RS, Dressano D, Braga RR, Aguiar FHB, & Marchi GM (2019) Effect of diphenyliodonium hexafluorophosphate salt on experimental infiltrants containing different diluents *Odontology* **107(2)** 202-208.
15. Yasa E, Yasa B, Aglarci OS, & Ertas ET (2015) Evaluation of the radiopacities of bulk-fill restoratives using two digital radiography systems *Operative Dentistry* **40(5)** E197-205. doi: 10.2341/14-074-L
16. Saridag S, Helvacioglu-Yigit D, Alniacik G, & Özcan M (2015) Radiopacity measurements of direct and indirect resin composites at different thicknesses using digital image analysis *Dental Materials Journal* **34(1)** 13-18. doi: 10.4012/dmj.2014-181
17. Ermis RB, Yildirim D, Yildiz G, & Gormez O. Radiopacity evaluation of contemporary resin composites by digitization of images *European Journal of Dentistry* **8(3)** 342-347. doi: 10.4103/1305-7456.137644
18. Pekkan G (2016) Radiopacity of dental materials: An overview *Avicenna Journal of Dental Research* **8(2)** e36847. doi: 10.17795/ajdr-36847
19. Lee JH, Um CM, & Lee IB (2006) Rheological properties of resin composites according to variations in monomer and filler composition *Dental Materials* **22(6)** 515-526.
20. Rueggeberg FA, Hashinger DT, & Fairhurst CW (1990) Calibration of FTIR conversion analysis of contemporary dental resin composites *Dental Materials* **6(4)** 241-249.
21. Vivan RR, Ordinola-Zapata R, Bramante CM, Bernardineli N, Garcia RB, Hungaro Duarte MA, & de Moraes IG (2009) Evaluation of the radiopacity of some commercial and experimental root-end filling materials *Oral Surgery Oral Medicine Oral Pathology Oral Radiology and Endodontology* **108(6)** e35-e38.
22. ten Cate JM & Duijsters PP (1982) Alternating demineralization and remineralization of artificial enamel lesions *Caries Research* **16(3)** 201-210.
23. Guerreiro Tanomaru JM, Storto I, Da Silva GF, Bosso R, Costa BC, Bernardi MI, & Tanomaru-Filho M (2014) Radiopacity, pH and antimicrobial activity of Portland cement associated with micro- and nanoparticles of zirconium oxide and niobium oxide *Dental Materials Journal* **33(4)** 466-470.
24. Groeneveld A & Arends J (1975) Influence of pH and demineralization time on mineral content, thickness of surface layer and depth of artificial caries lesions *Caries Research* **9(1)** 36-44.
25. Cochrane NJ, Anderson P, Davis GR, Adams GG, Stacey MA, & Reynolds EC (2012) An X-ray microtomographic study of natural white-spot enamel lesions *Journal of Dental Research* **91(2)** 185-191.
26. Braem M, Finger W, Van Doren VE, Lambrechts P, & Vanherle G (1989) Mechanical properties and filler fraction of dental composites *Dental Materials* **5(5)** 346-348.
27. Li Y, Swartz ML, Phillips RW, Moore BK, & Roberts TA (1985) Effect of filler content and size on properties of composites *Journal of Dental Research* **64(12)** 1396-1401.
28. Sfalcin RA, Correr AB, Morbidelli LR, Araújo TGF, Feitosa VP, Correr-Sobrinho L, Watson TF, & Sauro S (2017) Influence of bioactive particles on the chemical-mechanical properties of experimental enamel resin infiltrants *Journal of Clinical Oral Investigations* **21(6)** 2143-2151.
29. Dickens SH, Stansbury JW, Choi KM, & Floyd CJE (2003) Photopolymerization kinetics of methacrylate dental resins *Macromolecules* **36(16)** 6043-6053.
30. Gajewski VE, Pfeifer CS, Fróes-Salgado NR, Boaro LC, & Braga RR (2012) Monomers used in resin composites: degree of conversion, mechanical properties and water sorption/solubility *Brazilian Dental Journal* **23(5)** 508-514.
31. Lovell LG, Stansbury JW, Syrpes DC, & Bowman CN (1999) Effects of composition and reactivity on the reaction kinetics of dimethacrylate/dimethacrylate copolymerizations *Macromolecules* **32(12)** 3913-3921.
32. Neres ÉY, Moda MD, Chiba EK, Briso A, Pessan JP, & Fagundes TC (2017) Microhardness and roughness of infiltrated white spot lesions submitted to different challenges *Operative Dentistry* **42(4)** 428-435.
33. Halvorson RH, Erickson RL, & Davidson CL (2003) The effect of filler and silane content on conversion of resin-based composite *Dental Materials* **19(4)** 327-333.

34. Atai M & Watts DC (2006) A new kinetic model for the photopolymerization shrinkage-strain of dental composites and resin-monomers *Dental Materials* **22(8)** 785-791.

35. Inagaki LT, Dainezi VB, Alonso RC, Paula AB, Garcia-Godoy F, Puppin-Rontani RM, & Pascon FM (2016) Evaluation of sorption/solubility, softening, flexural strength and elastic modulus of experimental resin blends with chlorhexidine *Journal of Dentistry* **49** 40-45.

36. Bortoluzzi EA, Guerreiro-Tanomaru JM, Tanomaru-Filho M, & Duarte MA (2009) Radiographic effect of different radiopacifiers on a potential retrograde filling material *Oral Surgery Oral Medicine Oral Pathology Oral Radiology Endodontology* **108(4)** 628-632.

37. Verma R, Fischer BI, Gregory RL, & Yassen GH (2018) The radiopacity and antimicrobial properties of different radiopaque double antibiotic pastes used in regenerative endodontics *Journal of Endodontics* **44(9)** 1376-1380.

38. Watts DC (1987) Radiopacity vs. composition of some barium and strontium glass composites *Journal of Dentistry* **15(1)** 38-43.

39. van Dijken JW, Wing KR, & Ruyter IE (1989) An evaluation of the radiopacity of composite restorative materials used in Class I and Class II cavities *Acta Odontologica Scandinavica* **47(6)** 401-407.